Three-dimensional character of the Fermi surface in ultrathin $LaTiO_3/SrTiO_3$ heterostructures

M. J. Veit,[1] M. K. Chan,[2] B. J. Ramshaw,[2,3] R. Arras,[4] R. Pentcheva,[5] and Y. Suzuki[1]

[1]*Department of Applied Physics and Geballe Laboratory for Advanced Materials, Stanford University, Stanford, California 94305, USA*

[2]*Los Alamos National Laboratory, Los Alamos, New Mexico 87544, USA*

[3]*Laboratory for Atomic and Solid State Physics, Cornell University, Ithaca, New York 14853, USA*

[4]*CEMES, University of Toulouse, CNRS, UPS, 29, rue Jeanne Marvig, F-31055 Toulouse, France*

[5]*Department of Physics and Center for Nanointegration (CENIDE), University of Duisburg-Essen, Lotharstr. 1, 47057 Duisburg, Germany*

(Received 26 October 2018; revised manuscript received 4 February 2019; published 18 March 2019)

$LaTiO_3$ films on $SrTiO_3$ single crystal substrates exhibit metallic behavior attributed to the $LaTiO_3$ film, the interface as well as part of the $SrTiO_3$. In the limit of ultrathin $LaTiO_3$ films on $SrTiO_3$, the contribution to the metallicity from strain-induced electronic structure modification of the $LaTiO_3$ film is minimized so that the dominant contribution to metallicity is from the interface and part of the $SrTiO_3$ due to charge transfer of $3d$ electrons from $LaTiO_3$ to $SrTiO_3$. In such a limit, we observe quantum oscillations whose angular dependence indicates a three-dimensional Fermi surface. Such angular dependence is observed in two sets of quantum oscillations—one low frequency and one high frequency—that we have attributed to an inner and outer Fermi surface associated with a Rashba-like spin split hybridized d_{xz+yz} band.

DOI: 10.1103/PhysRevB.99.115126

I. INTRODUCTION

Emergent phenomena at complex oxide interfaces have largely been confined to the interface or a few unit cells near the interface. These oxide interfaces provide model systems for the study of low-dimensional metallicity, superconductivity, and ferromagnetism, and they have been almost systematically studied with mageotransport and electrical gating [1–4]. For example, δ-doped $SrTiO_3$ (STO) has shown strong evidence for 2D metallicity in the form of quantum oscillations which are easily suppressed as a function of the magnetic field orientation [5] and the quantum Hall effect [6]. At the spinel/perovskite interface of γ-Al_2O_3/STO, quantum oscillations show a $1/\cos(\theta)$ dependence with the direction of the magnetic field suggesting that it is 2D [7]. In the well-studied LAO/STO system, there have been some conflicting reports with some samples showing 3D conduction [8]—consistent with Nb-doped STO single crystals [9]—and others showing 2D conduction [10]. However, the majority of evidence points to the two dimensionality of this system.

However, the diversity of oxide systems studied with quantum oscillations is small due to the high electron mobility required to observe them. More specifically the mobility values need to be high enough such that $\omega_c\tau > 1$. Typically low temperatures and high magnetic fields are required to observe the quantum oscillations.

The $LaTiO_3/SrTiO_3$ (LTO/STO) system has been shown to have high mobilities [11,12], but quantum oscillations have only recently been observed in ultrathin (three unit cells) LTO films [13]. Bulk LTO is a Mott insulator close to a metal-insulator transition with a small band gap of 0.1 eV [14]. Metallicity in LTO can be induced by cation vacancies, excess oxygen, alkaline-earth doping of the rare-earth site and epitaxial strain [14–21]. Furthermore it has been shown that LTO juxtaposed with STO induces metallicity [11,12] and even superconductivity [22] at the interface, and it has been proposed that the system orders magnetically [23,24]. The observation of a range of emergent properties at the LTO/STO interface has led to analogies with the well-studied LAO/STO interface. However, there are some very important differences in the two systems.

First of all, LTO itself exhibits metallic behavior when deposited on STO single substrates under compressive epitaxial strain. In fact, it has previously been reported that the sheet resistance scales with the thickness of the LTO in LTO/STO structures which was used to show that the entirety of the film is conductive [11] with only a small portion of the conduction due to a reconstruction at the interface [12]. This bulk metallicity in the LTO is due to the fact that the epitaxial strain eliminates the Mott insulating gap [25]. In contrast, the bulk of the LAO film on STO remains insulating despite the LAO/STO interface exhibiting metallic behavior. Second of all, we have demonstrated a giant Rashba-like spin-orbit splitting in LTO/STO more than an order of magnitude larger than has been reported in LAO/STO [13]. Such a large spin-orbit interaction has been confirmed by (i) two sets of quantum oscillations associated with two high-mobility bands with effective masses that differ by an order of magnitude and a Berry phase of π, (ii) weak antilocalization correction to the magnetoconductivity, and (iii) large anisotropic magnetoresistance. We deduced that the giant Rashba coupling is associated with hybridized d_{xy+yz} orbitals by identifying the bands crossing the Fermi level from density functional theory (DFT) calculations.

In this paper, we demonstrate that the Fermi surface of ultrathin LTO films on STO has a three-dimensional character as evident in the angular dependence of the quantum oscillations. The three-dimensional character is surprising given the thickness of the LTO film. However, DFT calculations indicate that the Rashba split states responsible for the quantum oscillations are derived from STO hybridized d_{xy+yz} orbitals close to the interface which are nearly isotropic in the three

dimensions [13]. Through a combination of DFT calculations and a tight binding model with a Rashba coupling, we have modeled the Fermi surface of our ultrathin LTO films on STO which closely matches the measured angular dependence of the quantum oscillations.

II. EXPERIMENTAL METHODS

LTO films were grown on STO single crystal substrates by pulsed laser deposition (PLD). A KrF laser ($\lambda = 248$ nm) operated at a repetition rate of 1 Hz was incident upon a $La_2Ti_2O_7$ target with a fluence of 1.4 J/cm^2. The substrate was heated to 625 °C at the base chamber pressure of 10^{-6} Torr. Analysis with a residual gas analyzer showed that the approximate oxygen partial pressure in these conditions was $\sim 5 \times 10^{-7}$ Torr. Previous studies have shown that the $LaTiO_3$ phase can be stabilized on a substrate from a $La_2Ti_2O_7$ target under the appropriate conditions [26]. Commercially available (001)-oriented STO substrates from Crystec were used. Prior to the deposition, the substrates were treated by chemical etching to achieve a TiO_2-terminated surface [27], and then annealed at 1000 °C in atmosphere. The films were 1.2 nm thick as determined by extrapolating the growth rate from thicker films which could be measured by x-ray reflectivity to determine the thickness.

The electrical transport measurements were taken using a Hall bar geometry of dimensions 5 mm × 1 mm with ultrasonically wire-bonded aluminum wires as electrodes. The temperature and magnetic field dependence were measured in a Quantum Design Dynacool system from 2 to 300 K and up to an applied magnetic field of 9 T. Additionally, magnetoresistance measurements were performed up to 60 T at the National High Magnetic Field Laboratory of Los Alamos National Laboratory. Because the magnetoresistance is an even function of applied field, the resistance was averaged over positive and negative fields to remove any residual Hall effect in the longitudinal magnetoresistance measurements. Similarly, the difference between the Hall resistance at positive and negative fields was taken to remove any residual longitudinal magnetoresistance in the Hall effect measurements.

III. ELECTRONIC TRANSPORT

Longitudinal magnetoresistance measurements of our samples showed evidence for quantum oscillations in low magnetic fields between 1 T and 3 T (Fig. 1) and in high magnetic fields above about 30 T (Fig. 2). We previously showed the full temperature dependence of the amplitude and a full fit to the Lifshitz-Kosevich equation both of which match that of quantum oscillations which definitively shows that the both sets of oscillations are Shubnikov–de Haas oscillations [13]. Our previous studies have shown that these quantum oscillations are characteristic of the high mobility carriers (4000 cm^2/V s) present in our LTO/STO system [13]. Lower mobility carriers (46 cm^2/V s) are only evident in our Hall effect measurements (see Supplemental Material [28]). In order to probe the dimensionality of the Fermi surface, we have performed longitudinal magnetoresistance measurements for both low and high magnetic fields as a function of the angle of the magnetic field with respect to the film normal direction.

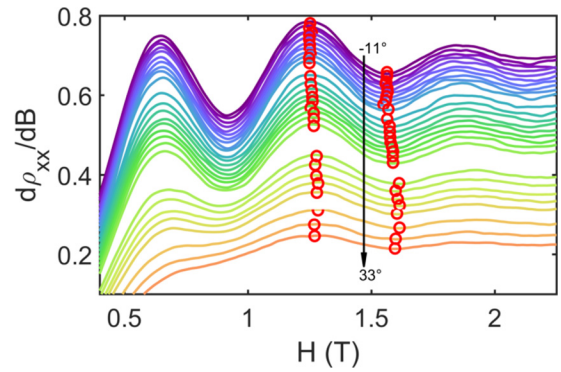

FIG. 1. Angular dependence of the low frequency oscillations. The angle of the magnetic field is measured with respect to the normal of the interface. Red circles indicate the extrema used to calculate the frequency.

Figures 1 and 2 show the angular dependences of the quantum oscillations in the longitudinal magnetoresistance with the background removed at 2 K (see Supplemental Material [29]). The frequency was calculated for each angle from the largest maximum oscillation and the closest minimum. This method was chosen because other methods for calculating the frequency such as taking the Fourier transform and indexing more extrema was difficult at higher angles because the amplitude decreases with increasing angle. Therefore, this method allows us to consistently calculate the frequency for all angles.

Angular dependent studies of these oscillations indicate that the frequency of the oscillations changes very little with the angle between the field and the crystallographic orientation. As the angle is changed from the field being perpendicular to the film to 40° away from perpendicular in a direction parallel to the current, the low frequency oscillations change by a negligible amount and the high frequency oscillations decrease from 39 T to 33 T. At angles greater than 40° away from perpendicular, the amplitude of the oscillations is too small to observe above the background. This is in sharp contrast with what is expected in two-dimensional systems. The frequency of quantum oscillations is related to the cross-sectional area of the Fermi surface perpendicular to the magnetic field by $F = \frac{\Phi_0}{2\pi}A$, where Φ_0 is the magnetic flux quantum, and in two-dimensional systems the Fermi surface is cylindrical. Therefore, the frequency should be proportional to $1/\cos(\theta)$

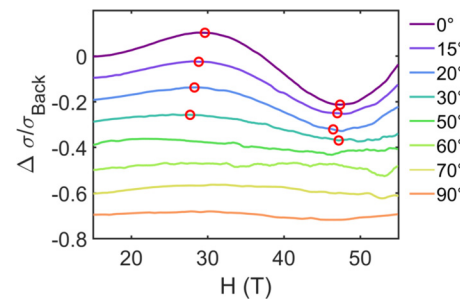

FIG. 2. Angular dependence of the high frequency oscillation. The given angle is measured from the normal of the interface. Red circles indicate the extrema used to calculate the frequency.

and increases with increasing angle for both the high and low frequency oscillations. However, our data indicate that the Fermi surface actually has some three-dimensional character because of its angular independence.

IV. TIGHT-BINDING MODEL

In order to model this angular dependence and its dimensionality, we apply the tight binding model for a hybridized d_{xz+yz} orbital which DFT calculations have indicated give rise to these oscillations [13]. For d_{xy+yz} orbitals, the tight binding Hamiltonian H of the system with nearest-neighbor hopping in the basis $\{d_I\}$, where $I = (X, Y)$ corresponds to the orbital character (yz, xz) of the two d orbitals, is given by [30]

$$H = (d_X \quad d_Y)\begin{pmatrix} \epsilon_X & \epsilon_{XY} \\ \epsilon_{XY} & \epsilon_Y \end{pmatrix}\begin{pmatrix} d_X \\ d_Y \end{pmatrix}, \tag{1}$$

with

$$\begin{aligned} \epsilon_X &= -2t_1\cos(ak_x) - 2t_2\cos(ak_y) - 2t_1\cos(ak_z), \\ \epsilon_Y &= -2t_2\cos(ak_x) - 2t_1\cos(ak_y) - 2t_1\cos(ak_z), \\ \epsilon_{XY} &= -2t_3[\cos(ak_x) + \cos(ak_y) + \cos(ak_z)]. \end{aligned} \tag{2}$$

A Rashba effect on top of this band structure requires adding an energy term $\epsilon_R = \alpha\sqrt{k_x^2 + k_y^2}$ to the diagonal elements. With this model, we deduce the angular dependence of the Fermi surface cross sectional area. The hopping terms t_1, t_2, and t_3, and the Fermi energy E_f were obtained by fitting these equations to the DFT calculations [13]. The Rashba constant was calculated to fit the cross-sectional area and effective masses measured from the two sets of quantum oscillations as described in Ref. [13]. Diagonalizing the resulting Hamiltonian and equating it to the Fermi energy produced the Fermi surface in k space. The maximum cross-sectional area perpendicular to the magnetic field was then calculated through numerical integration for a variety of field angles. Note that no further fitting to the experimental data was done to include the angular dependence. The results of this are shown in Fig. 3 as solid lines for the inner and outer Fermi surfaces with the experimental data in open circles. Clearly, this model fits well with the experimental data up to nearly 40°, where the amplitude of the oscillations becomes too small to measure. It is important to mention that the argument for three-dimensional behavior does not depend on the accuracy of this model. Because both frequencies lack a $1/\cos\theta$ dependence, both sets of oscillations independently show that the transport is not two dimensional.

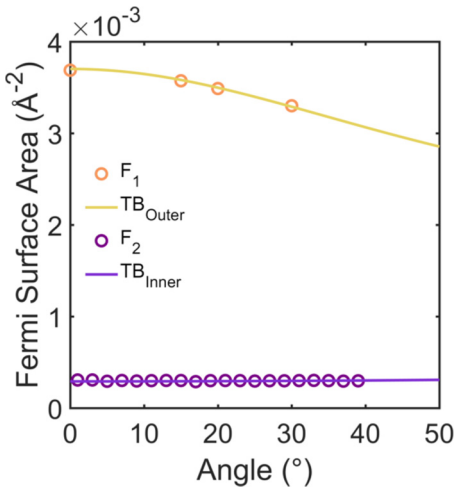

FIG. 3. Angular dependence of the Fermi surface area determined from the frequency of the oscillations. The circles represent the experimental data and the solid lines show the prediction from the tight binding model.

V. DISCUSSION

Because these films are so thin, it is surprising to observe a 3D Fermi surface so it is important to consider how this is possible. In a naive semiclassical approach, you can compare the classical orbits to the dimensions of the sample. The in-plane size of the sample is clearly much bigger than the cyclotron orbits so we must only consider the distance that the electron travels in the out-of-plane direction. Semiclassically, the radius of the smallest cyclotron orbit is the magnetic length, $l_b = \sqrt{\frac{\hbar}{eB}}$. So we can roughly estimate the thickness of the conducting portion of the heterostructure required to observe quantum oscillations with the field at an angle θ from the perpendicular direction to be $l_b \sin\theta$. For a maximum magnetic field of 60 T, the out-of-plane size of the orbit is 2.3 nm at 45°. This is on the order of the LTO film thickness so it could reasonably be understood that the conduction comes from the entirety of the film. However, oscillations are seen at much lower fields in our samples. At a field of 4 T, the out-of-plane size is 9 nm. This is significantly larger than the LTO film thickness suggesting that conduction also comes from within the STO side of the interface which is in agreement with DFT calculations.

Schrödinger-Poisson calculations of LTO/STO heterostructures have suggested that the electron gas extends nearly 6 nm into the STO in LTO/STO heterostructures [1,31,32]. However, the penetration depth has been studied extensively in the LAO/STO system, and a wide range of penetration depths have been reported [33–35]. It has even been suggested that the penetration depth can be several hundred nanometers at low carrier concentrations which would indeed make 3D conduction possible [33]. The 3D conduction observed here suggests that the penetration depth is much longer than the 6 nm previously predicted for the LTO/STO system. Therefore, the 3D conduction likely comes from an electron gas extending into the STO due to an electronic reconstruction at the interface.

Note that it is possible to reduce the STO substrate during the PLD process in low oxygen pressures causing it to become conductive [36]. Therefore, it is possible that the measured oscillations are actually in a thin layer of the substrate instead of the LTO film. However, by the same argument above, the thickness of this reduced layer would have to be approximately 1.5 nm thick to observe the 3D nature of the quantum oscillations. However, reduction of a single crystal STO substrate by annealing usually requires high temperatures (around 1000 °C), low oxygen pressures, and long annealing times (hours to days) [37–39]. Given the very short deposition time and the excess oxygen in the target, we find it very unlikely that there was enough reduction in

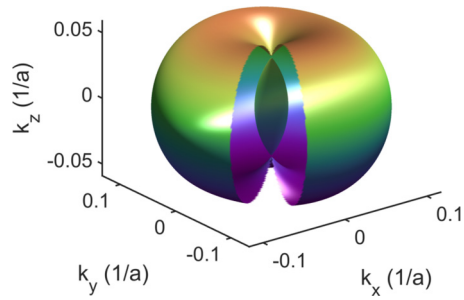

FIG. 4. Diagram of the proposed Fermi pocket. There is a cut through the outer Fermi pocket in order to visualize the smaller inner pocket.

the substrate to give rise to any conduction. To test whether our growth conditions reduced the substrate, we annealed a substrate in the growth conditions but observed insulating behavior. We also did a deposition with a $DyScO_3$ (DSO) target instead of LTO using the same conditions. These DSO films on STO substrates showed no conductivity. Additionally, the two-point resistance between the bottom of the substrate and the top surface of the film is greater than our measurement limit of 1 GΩ for both the DSO/STO and LTO/STO heterostructures. So we conclude that all of the conduction measured in the LTO/STO samples comes from the LTO film or the interface, and it is not a bulk STO substrate conduction that gives this 3D conduction.

In the LAO/STO system, it has been debated whether the high mobility quantum oscillations come from the Ti d_{xy} orbitals or the d_{xz}/d_{yz} orbitals; here we attribute the oscillations to the hybridized Ti d_{xy+yz} orbitals from DFT calculations discussed previously. The Fermi pocket formed from Ti d_{xy} orbitals in LAO/STO is isotropic in the plane of the film, but highly anisotropic in the z direction. Therefore, they would give a typical 2D-like dependence to the angular dependence of the quantum oscillations. On the other hand, hybridized Ti d_{xy+yz} orbitals are much more isotropic in all three directions—especially near the Γ point. Such an isotropic Fermi pocket is consistent with the angular dependence of the quantum oscillations observed here. (See Fig. 4.)

VI. CONCLUSIONS

In summary, we have observed quantum oscillations in ultrathin LTO/STO heterostructures that are nearly independent of the angle of the applied field with respect to the film up to ∼45°. This indicates that the Fermi surface is three dimensional rather than two dimensional as is found in other similar systems. These experimental results are consistent with a model that combines DFT calculations and a tight binding model with Rashba coupling to produce a model three-dimensional Fermi surface.

ACKNOWLEDGMENTS

This work was funded by the Vannevar Bush Faculty Fellowship of the Department of Defense under Contract No. N00014-15-1-0045. M.J.V. acknowledges a National Science Foundation Graduate Fellowship. Work at the National High Field Magnetic Laboratory was funded by the state of Florida, the Department of Energy, and the NSF Cooperative Agreement No. DMR-1157490. M.K.C. was supported by DOE-BES Science at 100T grant. This work was granted access to the HPC resources of the CALMIP supercomputing center under the allocation p1229. R.A. and R.P. acknowledge funding by the German Science Foundation within SFB/TRR 80 (Projects No. C03 and No. G03) and computational time at the Leibniz Rechenzentrum Garching, Project No. pr87ro.

[1] J. Biscaras, S. Hurand, C. Feuillet-Palma, A. Rastogi, R. Budhani, N. Reyren, E. Lesne, J. Lesueur, and N. Bergeal, Sci. Rep. **4**, 6788 (2014).

[2] S. Hurand, A. Jouan, C. Feuillet-Palma, G. Singh, J. Biscaras, E. Lesne, N. Reyren, A. Barthélémy, M. Bibes, J. Villegas *et al.*, Sci. Rep. **5**, 12751 (2015).

[3] J. S. Kim, S. S. A. Seo, M. F. Chisholm, R. K. Kremer, H.-U. Habermeier, B. Keimer, and H. N. Lee, Phys. Rev. B **82**, 201407 (2010).

[4] S. Seri, M. Schultz, and L. Klein, Phys. Rev. B **87**, 125110 (2013).

[5] B. Jalan, S. Stemmer, S. Mack, and S. J. Allen, Phys. Rev. B **82**, 081103 (2010).

[6] Y. Matsubara, K. Takahashi, M. Bahramy, Y. Kozuka, D. Maryenko, J. Falson, A. Tsukazaki, Y. Tokura, and M. Kawasaki, Nat. Commun. **7**, 11631 (2016).

[7] Y. Chen, N. Bovet, F. Trier, D. Christensen, F. Qu, N. H. Andersen, T. Kasama, W. Zhang, R. Giraud, J. Dufouleur *et al.*, Nat. Commun. **4**, 1371 (2013).

[8] G. Herranz, M. Basletić, M. Bibes, C. Carrétéro, E. Tafra, E. Jacquet, K. Bouzehouane, C. Deranlot, A. Hamzić, J.-M. Broto, A. Barthélémy, and A. Fert, Phys. Rev. Lett. **98**, 216803 (2007).

[9] H. P. R. Frederikse, W. R. Hosler, W. R. Thurber, J. Babiskin, and P. G. Siebenmann, Phys. Rev. **158**, 775 (1967).

[10] A. D. Caviglia, S. Gariglio, C. Cancellieri, B. Sacépé, A. Fête, N. Reyren, M. Gabay, A. F. Morpurgo, and J.-M. Triscone, Phys. Rev. Lett. **105**, 236802 (2010).

[11] F. J. Wong, S.-H. Baek, R. V. Chopdekar, V. V. Mehta, H.-W. Jang, C.-B. Eom, and Y. Suzuki, Phys. Rev. B **81**, 161101 (2010).

[12] C. He, T. D. Sanders, M. T. Gray, F. J. Wong, V. V. Mehta, and Y. Suzuki, Phys. Rev. B **86**, 081401 (2012).

[13] M. Veit, R. Arras, B. Ramshaw, R. Pentcheva, and Y. Suzuki, Nat. Commun. **9**, 1458 (2018).

[14] T. Arima, Y. Tokura, and J. B. Torrance, Phys. Rev. B **48**, 17006 (1993).

[15] Y. Okada, T. Arima, Y. Tokura, C. Murayama, and N. Mori, Phys. Rev. B **48**, 9677 (1993).

[16] Y. Tokura, Y. Taguchi, Y. Okada, Y. Fujishima, T. Arima, K. Kumagai, and Y. Iye, Phys. Rev. Lett. **70**, 2126 (1993).

[17] C. C. Hays, J.-S. Zhou, J. T. Markert, and J. B. Goodenough, Phys. Rev. B **60**, 10367 (1999).
[18] Y. Okimoto, T. Katsufuji, Y. Okada, T. Arima, and Y. Tokura, Phys. Rev. B **51**, 9581 (1995).
[19] C. Eylem, Y.-C. Hung, H. Ju, J. Kim, D. Green, T. Vogt, J. Hriljac, B. Eichhorn, R. Greene, and L. Salamanca-Riba, Chem. Mater. **8**, 418 (1996).
[20] T. Katsufuji, Y. Taguchi, and Y. Tokura, Phys. Rev. B **56**, 10145 (1997).
[21] T. Higuchi, D. Baba, T. Takeuchi, T. Tsukamoto, Y. Taguchi, Y. Tokura, A. Chainani, and S. Shin, Phys. Rev. B **68**, 104420 (2003).
[22] J. Biscaras, N. Bergeal, A. Kushwaha, T. Wolf, A. Rastogi, R. Budhani, and J. Lesueur, Nat. Commun. **1**, 89 (2010).
[23] S. Okamoto and A. J. Millis, Nature (London) **428**, 630 (2004).
[24] S. Okamoto, A. J. Millis, and N. A. Spaldin, Phys. Rev. Lett. **97**, 056802 (2006).
[25] H. Ishida and A. Liebsch, Phys. Rev. B **77**, 115350 (2008).
[26] A. Ohtomo, D. A. Muller, J. L. Grazul, and H. Y. Hwang, Appl. Phys. Lett. **80**, 3922 (2002).
[27] M. Kawasaki, K. Takahashi, T. Maeda, R. Tsuchiya, M. Shinohara, O. Ishiyama, T. Yonezawa, M. Yoshimoto, and H. Koinuma, Science **266**, 1540 (1994).
[28] See Supplemental Material at http://link.aps.org/supplemental/10.1103/PhysRevB.99.115126 for the Hall effect at 2K in Supplemental Note 1.
[29] See Supplemental Material at http://link.aps.org/supplemental/10.1103/PhysRevB.99.115126 for the raw magnetoresistance data prior to removing the background in Supplemental Note 2.
[30] Z. Zhong, A. Tóth, and K. Held, Phys. Rev. B **87**, 161102 (2013).
[31] J. Biscaras, N. Bergeal, S. Hurand, C. Grossetête, A. Rastogi, R. C. Budhani, D. LeBoeuf, C. Proust, and J. Lesueur, Phys. Rev. Lett. **108**, 247004 (2012).
[32] W. Meevasana, P. King, R. He, S. Mo, M. Hashimoto, A. Tamai, P. Songsiriritthigul, F. Baumberger, and Z. Shen, Nat. Mater. **10**, 114 (2011).
[33] O. Copie, V. Garcia, C. Bödefeld, C. Carrétéro, M. Bibes, G. Herranz, E. Jacquet, J.-L. Maurice, B. Vinter, S. Fusil *et al.*, Phys. Rev. Lett. **102**, 216804 (2009).
[34] A. Janotti, L. Bjaalie, L. Gordon, and C. G. Van de Walle, Phys. Rev. B **86**, 241108 (2012).
[35] S. Gariglio, A. Fête, and J.-M. Triscone, J. Phys.: Condens. Matter **27**, 283201 (2015).
[36] M. L. Scullin, J. Ravichandran, C. Yu, M. Huijben, J. Seidel, A. Majumdar, and R. Ramesh, Acta Mater. **58**, 457 (2010).
[37] H. Frederikse, W. Thurber, and W. Hosler, Phys. Rev. **134**, A442 (1964).
[38] V. E. Henrich, G. Dresselhaus, and H. J. Zeiger, Phys. Rev. B **17**, 4908 (1978).
[39] C. Lee, J. Yahia, and J. Brebner, Phys. Rev. B **3**, 2525 (1971).